Nanoscale amorphization at disclination quadrupoles in deformed nanomaterials and polycrystals

S. V. Bobylev and I. A. Ovid'ko[a)]
Institute of Problems of Mechanical Engineering, Russian Academy of Sciences, Bolshoj 61, Vasilievskii Ostrov, St. Petersburg 199178, Russia

(Received 9 May 2008; accepted 11 June 2008; published online 12 August 2008)

Special micromechanism of nanoscale amorphization (crystal-to-glass transition in nanoscale regions) in deformed nano- and polycrystalline materials is suggested and theoretically described. The nanoscale amorphization occurs through transformation of disclination quadrupoles generated during plastic deformation. It is shown that the nanoscale amorphization at disclination quadrupoles is energetically favorable in nano- and polycrystalline Si and Si_3N_4 deformed at high applied stresses in certain ranges of their structural parameters. © *2008 American Institute of Physics*. [DOI: 10.1063/1.2953448]

Following experimental data, computer simulations, and theoretical models,[1–20] nano- and polycrystalline materials deformed at very high stresses often show the specific behaviors. Of particular interest is the phenomenon of amorphization or, in other terms, crystal-to-glass transition occurring in nano- and polycrystalline materials deformed under shock-wave deformation, indenter load and ball milling; see, e.g., Refs. 2–4, 9, and 15–17. Sometimes, chemical factors are significantly involved in amorphization processes in deformed solids.[2,3] At the same time, there are several examples where chemical factors do not operate, and only extra high levels of elastic strains and stresses play the crucial role in driving the amorphization.[4,9,15–17] For instance, the experimentally observed formation of nanoscale intragranular amorphous bands that occur parallel to specific crystallographic planes in shock-loaded B_4C polycrystals can be attributed to a sudden collapse of the lattice due to the stress-induced loss of shear rigidity.[16] In other cases, plastic deformation in coarse-grained polycrystals is supposed to create high-density ensembles of defects (point defects, dislocations, twins, and sub-boundaries), and the crystal structure in some local regions transforms into the amorphous structure when the energy of a crystal with defects in these regions increases up to the energy of the amorphous state.[18] In nanocrystalline materials, generation and evolution of defects during plastic deformation are essentially different from those in their coarse-grained counterparts.[5–14,21,22] For instance, densities of point defects and dislocations in grain interiors are commonly very low because grain boundaries (GBs) effectively absorb point defects[21,22] and lattice dislocations.[8,12] In this context, there is large interest in identification of micromechanisms of experimentally observed[9,17] amorphization in deformed nanomaterials. The main aim of this paper is to suggest and theoretically describe a special amorphization micromechanism effectively operating in both nanomaterials and polycrystals. The micromechanism represents nanoscale amorphization through transformations of GB disclinations (line defects associated with abrupt changes/gaps in GB misorientation[23,24]) intensively generated in both polycrystals and especially nanomaterials deformed at high stresses.

In parallel with lattice dislocation slip, GB sliding, Coble creep, stress-driven twinning, and rotational deformation are considered as deformation modes significantly contributing to plastic flow in nanocrystalline materials,[6–8,10–14] Following theoretical models,[7,10,11,14] the rotational deformation (plastic flow associated with crystal lattice rotations) in nanomaterials involves formation and evolution of wedge disclinations. Such disclinations were experimentally observed in iron under ball-mill treatment resulting in the nanostructure formation[25] as well as in deformed coarse-grained polycrystals; see review[23] and references therein. Within the theoretical approach,[7,10,14] disclinations form nanoscale quadrupole configurations in deformed nanomaterials, in particular, during stress-driven migration of GBs (Ref. 7) [Fig. 1(a)], GB-sliding-initiated rotational deformation[11] [Fig. 1(b)], and nanograin nucleation[14] [Fig. 1(c)]. At the same time, the formation of disclination quadrupoles in nanomaterials is still awaiting experimental verification.

A wedge disclination quadrupole creates high elastic stresses within the crystalline rectangular area [ABCD in Fig. 1(c)] bounded by the disclinations,[23] while its stresses outside the rectangular area are comparatively low. The

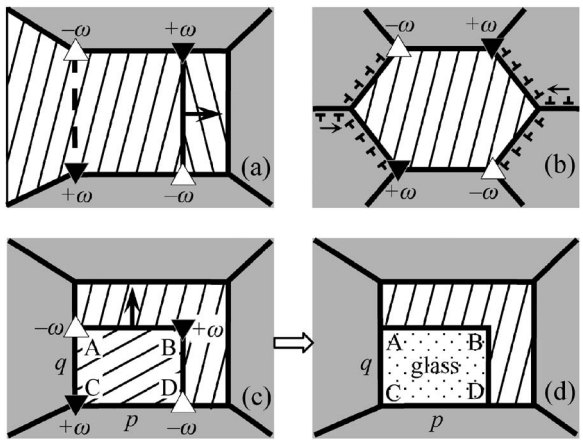

FIG. 1. Wedge disclination quadrupoles and amorphization in deformed nanomaterials. Formation of quadrupole of disclinations (triangles) during (a) stress-driven migration of GBs, (b) GB-sliding-initiated rotational deformation, and (c) nanograin nucleation. (d) Amorphization occurs in nanoscale region ABCD due to transformation of initial disclinations shown in (c).

a)Electronic mail: ovidko@def.ipme.ru.

stress level within the rectangular area is close to that created by an isolated disclination in a nanowire. Following computer simulations,[26] the disclination line core in a nanowire can spread into the nanoscale amorphous zone, and this nanoscale amorphization is driven by a decrease in the disclination strain energy.[26] In the context discussed, we think that the amorphization can also occur in a nanoscale rectangular area bounded by the disclinations generated during plastic deformation in nanomaterials, as shown in Figs. 1(c) and 1(d). In this transformation, the disclinations spread into the amorphous area ABCD. The stresses created by the initial disclination quadrupole in the rectangular area ABCD [Fig. 1(c)] relax, and the corresponding decrease in the elastic energy drives the amorphization. On the other hand, the amorphous region ABCD [Fig. 1(d)] is characterized by a positive difference in the energy between the amorphous and crystalline phases, and this difference hampers the amorphization process. Also, the amorphization is accompanied by formation of the crystal/glass interface ABCD [Fig. 1(d)] which replaces pre-existent GBs [Figs. 1(a)–1(c)]. That is, the amorphization leads to transformation of GBs into the crystal/glass interface. The transformation either drives or hampers the amorphization, depending on the energies of the interfaces involved in it.

Let us calculate a change ΔW in the total energy of the system due to the amorphization in the nanoscale area ABCD [Figs. 1(c) and 1(d)]. The system in its initial state contains a disclination quadrupole specified by sizes p and q and by the disclination strengths $\pm\omega$ [Fig. 1(c)]. The energy change ΔW (per unit of disclination length) has the three terms:

$$\Delta W = \Delta g_\nu pq + \Delta W_i - W_{\mathrm{el}}^q, \tag{1}$$

where Δg_ν is the difference in the energy (per unit volume) between the amorphous and crystalline phases, ΔW_i is the difference in the energy of interfaces due to their transformation, and W_{el}^q is the elastic energy of the initial disclination quadrupole. The latter is calculated in the standard way[23] as follows:

$$W_{\mathrm{el}}^q = \frac{G\omega^2}{4\pi(1-\nu)}\left[p^2 \ln\frac{p^2+q^2}{p^2} + q^2 \ln\frac{p^2+q^2}{q^2}\right], \tag{2}$$

where G is the shear modulus and ν is the Poisson's ratio.

In order to calculate the interface energy change ΔW_i, one needs to identify the initial configuration of interfaces of the region ABCD [Fig. 1(c)]. Below we will consider the two typical cases. (i) The region ABCD in its initial state is bounded by four *general* GBs AB, BC, CD, and DA [Fig. 1(c)]. They are characterized by the specific energy (per unit area of interface) γ_{gb}. After amorphization [Fig. 1(d)], these GBs transform into crystal-glass interface ABCD characterized by the specific energy (per unit area of interface) γ_{a-c}. (ii) The region ABCD in its initial state is bounded by four *special* boundaries whose specific energies are low and can be neglected in a first approximation. After amorphization, crystal-glass interface ABCD characterized by the specific energy (per unit area of interface) γ_{a-c} is formed.

In the case (i), the interface energy change ΔW_i is given as

$$\Delta W_i = 2(p+q)(\gamma_{a-c} - \gamma_{gb}). \tag{3}$$

Here $2(p+q)$ is the sum length of all interfaces bounding the area ABCD. In case (ii), we have $\gamma_{gb}=0$, and the interface energy change ΔW_i is as follows:

$$\Delta W_i = 2(p+q)\gamma_{a-c}. \tag{4}$$

Substitution of formulas (2)–(4) into the expression (1), with values of parameters Δg_ν, γ_{a-c}, and γ_{gb} taken from either the corresponding experiments or computer simulations, allows one to calculate the total energy change ΔW characterizing the nanoscale amorphization (Fig. 1).

Let us calculate the energy change ΔW in the scientifically and technologically important cases of silicon (Si) and silicon nitride (Si_3N_4). In our calculations, for Si, we use the following typical values of the parameters: $G=68.1$ GPa, $\nu=0.218$,[27] $\Delta g_\nu=0.100$ eV/atom, and $\gamma_{a-c}=0.102$ eV/atom.[28,29] Since the mean interatomic distance in Si is 0.27 nm,[29] one finds the energies Δg_ν and γ_{a-c} per unit volume and unit area, respectively, to be given as $\Delta g_\nu = 8.13\times10^8$ J/m^3 and $\gamma_{a-c}=0.231$ J/m^2.[29] The energy γ_{gb} of general GBs is taken from computer simulations[30] of the energy of symmetric tilt boundaries in Si. The simulations[30] show the typical energy $\gamma_{gb}\approx 1$ J/m^2 of general GBs. With these values of γ_{a-c} and γ_{gb}, for Si, one finds that the interface energy change ΔW_i, given by formula (3), is always negative, while ΔW_i, given by formula (4), is always positive.

In our calculations concerning Si_3N_4, we use the following typical values of the parameters:[31] $G=119$ GPa, $\nu=0.2$, and the energy[32] $\Delta g_\nu=9.86$ kJ/mol or (in units of J/m^3) $\Delta g_\nu=1.69\times10^9$ J/m^3. For Si_3N_4, we have not found values of the energies γ_{a-c} and γ_{gb} in the literature. In these circumstances, in our calculations, we use the interface energy change ΔW_i written through a model parameter γ^* as follows: $\Delta W_i=2(p+q)\gamma^*$, where values of γ^* are taken from some reasonable range.

Figures 2(a) and 2(b) present the dependences $\Delta W(p)$ characterizing Si and Si_3N_4, respectively, for $q=5$ nm and various values of the disclination strength ω. For both Si and Si_3N_4, the calculation was performed in the case of $\Delta W_i<0$. For Si, we used formula (3), while, for Si_3N_4, the parameter γ^* was taken as $\gamma^*=-0.5$ J/m^2. Curves 1, 2, 3, and 4 in Fig. 2 correspond to values of $\omega=0.2$, 0.3, 0.4, and 0.5, respectively. The dependences $\Delta W(p)$ are calculated in the range of $p>2$ nm because lower values of p correspond to the situation where the disclinations are very close to each other and use of the continuum theory of disclinations is hardly relevant. To describe this situation, atomistic simulations are needed which are beyond the scope of our continuum approach.

The dependences in Fig. 2 show that, for any value of p, with rising the disclination strength ω, the total energy change ΔW gradually decreases and becomes negative at some critical value of $\omega=\omega_c$. (For small enough p, we have $\Delta W<0$ at any value of ω [Fig. 2(a)], in which case $\omega_c=0$.) The critical value of $\omega=\omega_c$ is found from the relationship $\Delta W=0$ as follows:

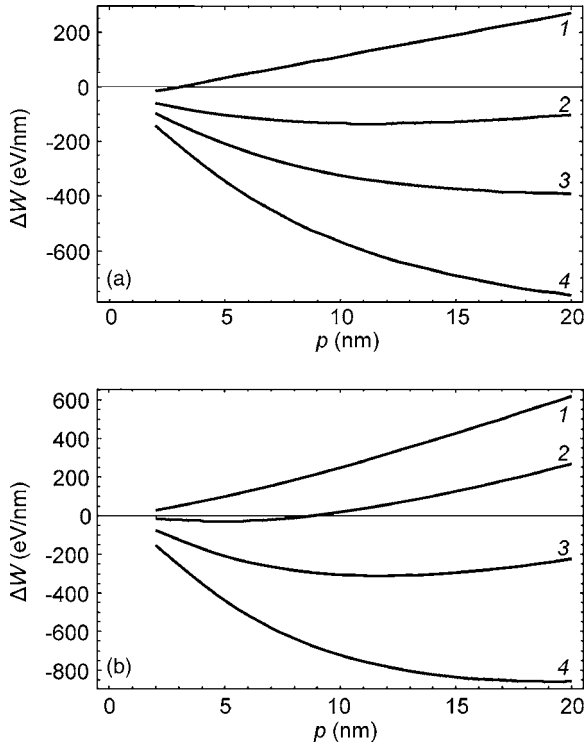

FIG. 2. Dependences of the total energy change ΔW on the disclination quadrupole size p in (a) Si and (b) Si_3N_4. Curves 1, 2, 3, and 4 correspond to values of ω=0.2, 0.3, 0.4, and 0.5, respectively.

$$\omega_c = \left\{ \frac{4\pi(1-\nu)(\Delta g_\nu pq + \Delta W_i)}{G[p^2 \ln(q^2/p^2+1) + q^2 \ln(p^2/q^2+1)]} \right\}^{1/2}. \quad (5)$$

The nanoscale amorphization (Fig. 1) is energetically unfavorable, if $\omega < \omega_c$, and favorable otherwise.

Figure 3 presents the dependences $\omega_c(p)$, given by formula (5), for Si. Solid and dashed curves in Fig. 3 correspond to the interface energy change ΔW_i, calculated by formulas (3) and (4), respectively. From Fig. 3, it follows that the critical disclination strength $\omega_c < 0.5$, for any reasonable values of p. Such strength values are typical for deformation-produced disclinations in nanomaterials.[7,10,14] A similar situation occurs with silicon nitride. For Si_3N_4, we calculated the dependences $\omega_c(p)$ and found that the critical disclination strength $\omega_c < 0.5$, when the interface energies and p are taken in reasonable ranges.

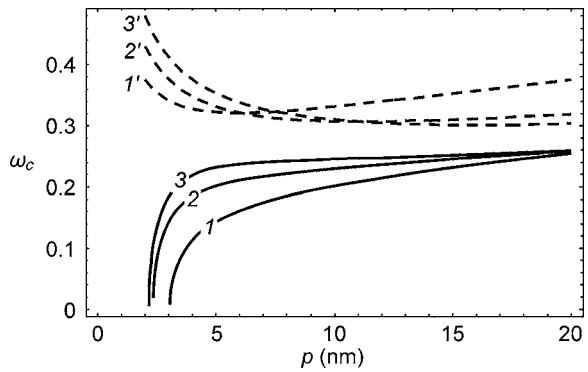

FIG. 3. Dependences of the critical disclination strength ω_c on disclination quadrupole size p in Si. Solid and dashed curves correspond to the interface energy change ΔW_i, calculated by formulas (3) and (4), respectively. Curves 1, 2, and 3 (1′, 2′, and 3′) correspond to values of q=5, 10 and 15 nm, respectively.

To summarize, with theoretical results of this paper, nanoscale amorphization in deformed nanomaterials and polycrystals can effectively occur as a process associated with transformations of deformation-produced disclination quadrupoles (Fig. 1). Here it has been shown that the nanoscale amorphization is energetically favorable in nano- and polycrystalline Si and Si_3N_4 deformed at high applied stresses in certain ranges of their structural parameters. In particular, the nanoscale amorphization effectively occurs through transformations of disclination quadrupoles (Fig. 1) in Si and Si_3N_4, if the disclination strength exceeds its critical value ω_c.

The work was supported, in part, by the Russian Federal Agency of Science and Innovations (Contract No. 02.513.11.3190 of the Program "Industry of Nanosystems and Materials" and Grant No. NSh-2405.2008.1), the National Science Foundation (Grant No. CMMI #0700272), the Russian Foundation of Basic Research (Grant No. 08-01-00225-a), and Russian Academy of Sciences Program "Structural Mechanics of Materials and Construction Elements."

[1] C. C. Koch, J. Mater. Sci. **42**, 1403 (2007).
[2] R. B. Schwarz and C. C. Koch, Appl. Phys. Lett. **49**, 146 (1986).
[3] K. Omuro and H. Miura, Appl. Phys. Lett. **64**, 2961 (1994).
[4] P. R. Okamoto, J. K. Heuer, N. Q. Lam, S. Ohnuki, Y. Matsukawa, K. Tozawa, and J. F. Stubbins, Appl. Phys. Lett. **73**, 473 (1998).
[5] Y. M. Wang and E. Ma, Appl. Phys. Lett. **83**, 3165 (2003); **85**, 2750 (2004).
[6] G.-D. Zhan, J. E. Garay, and A. K. Mukherjee, Nano Lett. **5**, 2593 (2005).
[7] M. Yu. Gutkin and I. A. Ovid'ko, Appl. Phys. Lett. **87**, 251916 (2005).
[8] D. Wolf, V. Yamakov, S. R. Phillpot, A. K. Mukherjee, and H. Gleiter, Acta Mater. **53**, 1 (2005).
[9] Y. M. Wang, E. M. Bringa, J. M. McNaney, M. Victoria, A. Caro, A. M. Hodge, R. Smith, B. Torralva, B. A. Remington, C. A. Schuh, H. Jamarkani, and M. A. Meyers, Appl. Phys. Lett. **88**, 061917 (2006).
[10] M. Yu. Gutkin, I. A. Ovid'ko, and N. V. Skiba, Phys. Rev. B **74**, 172107 (2006).
[11] M. Yu. Gutkin, I. A. Ovid'ko, and N. V. Skiba, Acta Mater. **51**, 4059 (2003).
[12] M. Dao, L. Lu, R. J. Asaro, J. T. M. De Hosson, and E. Ma, Acta Mater. **55**, 4041 (2007).
[13] Y. Mo and I. Szlufarska, Appl. Phys. Lett. **90**, 181926 (2007).
[14] S. V. Bobylev and I. A. Ovid'ko, Appl. Phys. Lett. **92**, 081914 (2008).
[15] Y. Q. Wu, X. Y. Yang, and Y. B. Xu, Acta Mater. **47**, 2431 (1999).
[16] M. Chen, J. W. McCauley, and K. J. Hemker, Science **299**, 1563 (2003).
[17] J. Li, Z. Q. Jin, J. P. Liu, Z. L. Wang, and N. N. Thadhani, Appl. Phys. Lett. **85**, 2223 (2004).
[18] E. Ma, Scr. Mater. **49**, 941 (2003).
[19] A. C. Lund and C. A. Schuh, Appl. Phys. Lett. **82**, 2017 (2003).
[20] I. Szlufarska, R. K. Kalia, A. Nakano, and P. Vashishta, Appl. Phys. Lett. **85**, 378 (2004).
[21] I. A. Ovid'ko and A. G. Sheinerman, Appl. Phys. A **81**, 1083 (2005).
[22] T. D. Chen, S. Feng, M. Tang, J. A. Valdez, Y. Wang, and K. Sickafus, Appl. Phys. Lett. **90**, 263115 (2007).
[23] A. E. Romanov, Eur. J. Mech. A/Solids **22**, 727 (2003).
[24] M. Kleman and J. Friedel, Rev. Mod. Phys. **80**, 61 (2008).
[25] M. Murayama, J. M. Howe, H. Hidaka, and S. Takaki, Science **295**, 2433 (2002).
[26] K. Zhou, A. A. Nazarov, and M. S. Wu, Phys. Rev. Lett. **98**, 035501 (2007).
[27] J. P. Hirth and J. Lothe, *Theory of Dislocations* (Wiley, New York, 1982).
[28] C. Spinella, S. Lombardo, and F. Priolo, J. Appl. Phys. **84**, 5383 (1998).
[29] M. Zacharias and P. Streitenberger, Phys. Rev. B **62**, 8391 (2000).
[30] M. Kohyama, Modell. Simul. Mater. Sci. Eng. **10**, R31 (2002).
[31] A. Khan, J. Philip, and P. Hess, J. Appl. Phys. **95**, 1667 (2004).
[32] R. F. Zhang and S. Veprek, Phys. Rev. B **76**, 174105 (2007).